

UDC 621.317.3:53.082.73

Electrical Impedance Mathematical Modeling of Piezoceramic Disc Oscillating in Wide Frequency Range (Part 3. High Frequencies)

Bazilo C. V.¹, Usyk L. M.¹, Khyzhniak Y. V.¹, Zhuikov D. B.², Yaroslaskyi A. V.¹

¹Cherkasy State Technological University, Cherkasy, Ukraine

²Ivan Kozhedub Kharkiv National Air Force University, Kharkiv, Ukraine

E-mail: k.bazilo@chdtu.edu.ua

This paper discusses the results of mathematical modelling the electrical impedance of a piezoceramic disk oscillating in a wide range of high frequencies. The study aimed to create a mathematical model that would incorporate geometric, physical, and mechanical characteristics of the material to assess the behavior of the disk under conditions of electromechanical resonance and antiresonance. The research particularly focused on the influence of radial and axial displacements of material particles on the frequency dependence of the mechanical quality factor and electrical impedance of the disk. Even more closely, this research scrutinizes specific effects characteristic of the high-frequency mode, in order to increase the accuracy of modeling and ensure optimal technical characteristics of the devices. The mathematical model developed in this paper serves as a tool to obtain estimates for the frequency dependence of the mechanical quality factor and the dynamic electrical capacitance in real conditions, in particular, by including energy losses due to viscous friction into the calculations. Numerical calculations confirm the high correlation between theoretical and experimental data (with the discrepancy lower than $3 \cdot 10^{-3}$), which proves the model usable for designing piezoelectric devices. In particular, it was found that the frequencies of electromechanical resonance and antiresonance are virtually independent of the radial displacements of material particles and are determined by the axial components solely. In addition, the calculation model provides the ability to assess the electrical impedance in the high-frequency range with an accuracy that meets modern requirements for the design of functional piezoelectric devices. The results obtained have practical significance for developing precision elements for military equipment, high-precision sensors, ultrasonic generators, medical diagnostic devices, and other technological systems that function with piezoelectric materials.

Keywords: electrical impedance; piezoceramic disk; high frequencies; mathematical modeling; mechanical quality factor; electromechanical resonance

DOI: [10.20535/RADAP.2025.99.15-23](https://doi.org/10.20535/RADAP.2025.99.15-23)

Introduction

Mathematical modeling of the electrical impedance of piezoceramic disks operating in a wide frequency range is an increasingly important area in today's scientific research, being widely applied in modern technology, in particular, in high-frequency modes. Piezoceramic disks are key elements in ultrasonic industrial devices, military equipment, sensors, actuators, medical ultrasound devices, as well as in non-destructive material testing systems [1]. Nonetheless, piezoceramic elements operating in high frequencies require a deeper insight into their electromechanical properties, which allows for the effective development of devices with high precision and stable operation.

Mathematical modeling, the results of which are considered in this article, is fast becoming a key

instrument in meeting the increasing requirements for the accuracy of modeling and calculating the electrical impedance. The efficiency of devices based on piezoelectric ceramic elements relies greatly on the results of mathematical modeling, which makes the studies in this field urgent and relevant. Failure to consider high-frequency effects can lead to design errors, reduced sensor sensitivity, or even device failure [2]. For instance, in high-frequency oscillation modes, complex electromechanical interactions arise that cannot be described without detailed mathematical analysis.

The research problem that we attempt to solve by this study includes nonlinearities and specific effects that arise in piezoceramic disks at high frequencies. Not only does this approach allow us to predict system behavior, but to optimize device design as well. Recent developments [3, 4] claim that accurate mathemati-

cal modeling of electrical impedance shortens the development cycle, improves the product quality, and reduces testing costs.

Therefore, mathematical modeling of the electrical impedance of a piezoceramic disk oscillating in a wide range of high frequencies may be applied to solve important applied problems, including determining the optimal design parameters of piezoceramic disks, predicting their resource, and increasing operating efficiency in a wide range of frequencies.

1 Topicality of the research based on the literature review

Mathematical modeling of electrical impedance in the high ultrasound frequency range is a narrow field of research that combines aspects of bioelectrical impedance tomography and ultrasound diagnostics. Today, a large and growing cohort of investigators are engaged in solving the problems of mathematical modeling of electrical impedance. In the pages that follow, we will review several most prominent and relevant studies in this field.

A study of particular interest is by Habib Ammari, Professor of Applied Mathematics [5], whose research delves into mathematical analysis and numerical methods for ultrasound-induced electrical conductivity tomography.

Pol Grasland-Mongrain [6], whose area of interest lies in the field of biomedical engineering, collaborates with Habib Ammari on mathematical models for applied issues of ultrasound-induced electrical conductivity tomography.

Research by Bastian Gebauer and Otmar Scherzer [7] has presented a hybrid imaging technique that combines electrical impedance tomography with acoustic tomography. This approach exploits the phenomenon in which the electrical energy absorbed within a body increases its temperature, leading to thermal expansion that in its turn generates acoustic waves. By analyzing these acoustic signals, researchers are able to determine the internal distribution of absorbed electrical energy, and therefore the body's electrical conductivity. This method aims to combine the high contrast of electrical impedance tomography with the high spatial resolution of ultrasound imaging.

In Ukraine, mathematical modeling of the electrical impedance of piezoceramic disks is the topic that is being actively explored by a number of research teams. In particular, at the National Technical University of Ukraine "Igor Sikorsky Kyiv Polytechnic Institute," which is one of the leading research centers in this field, a team of scientists led by Professor Yuriy Poplavko is developing innovative modeling and analysis methods that investigate, among other issues, piezoceramic disks [8].

G. E. Pukhov Institute for Modelling in Energy Engineering and I. M. Frantsevych Institute for Problems in Materials Science (National Academy of Sciences of Ukraine) are another prominent research centers of Ukraine that conducts fundamental research into the properties of piezoceramic materials and searches for innovative approaches to their mathematical modeling. For instance, a school of academics led by Professor Halyna Oleynyk, is developing theoretical and practical solutions for the use of ceramic piezomaterials in various devices [9].

As recent literature in the field suggests, mathematical modeling of the electrical impedance of piezoceramic disks is a subject of intensive and extensive research both in the international and Ukrainian academic community. The results to be obtained guarantee and foster scientific achievements in radio engineering, instrument making, medical technologies and other areas where accurate and reliable methods of analyzing and controlling piezoelectric materials are critically relevant.

In view of the above, mathematical modeling of the electrical impedance of a piezoceramic disk in the high-frequency range is an extremely relevant and promising topic, given the ongoing technological progress and the growing demand for high-precision instruments for various industries.

The purpose of the article is to develop a mathematical model of the electrical impedance of a piezoceramic disk oscillating in the high-frequency range for an accurate analysis of its electromechanical behavior.

2 Mathematical modeling of a piezoceramic disk transducer in the high-frequency range

Let us consider a disk with radius R which exceeds significantly its thickness α . The disk is located in a cylindrical coordinate system, where the coordinates (ρ, ϕ, z) determine its position, Fig. 1. The starting point of this coordinate system coincides with the center of the lower surface of the disk. The surfaces of the disk at heights $z = 0$ and $z = \alpha$ are electrodes. In this case, the piezoelectric disk is made of ceramics of the "lead zirconate-titanate" class with thickness α . The disk surfaces are covered with a thin layer of silver (up to 0.01 mm) by thermal vacuum deposition technology [10]. The lower surface of the disk ($z = 0$) has zero potential, i.e., it is grounded, and an electric potential $U_0 e^{i\omega t}$ is applied to the upper surface $z = \alpha$ under the condition of ensuring the electric field strength $U_0/\alpha \ll 0,1 E_0$ in the polarizing material of the disk, where U_0 is the amplitude value of the electric potential; $i = \sqrt{-1}$ is an imaginary unit, ω denotes angular frequency of sign inversion in the potential, t is duration of an oscillation cycle. The value

of such a potential is selected under the condition that guarantees the absence of nonlinear effects.

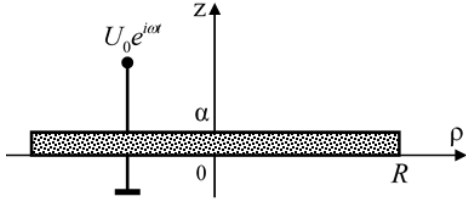


Fig. 1. Calculation model of a piezoceramic disk oscillating in a high-frequency range

Within the high-frequency range, where the elastic wavelength becomes commensurate with the thickness of the disk, the displacement vector of material particles has both radial and axial components. The electrical impedance of the oscillating piezoceramic disk will be determined as discussed in [11, 12].

Radial component $u_\rho^{(z)}(\rho)$ of the material particles' displacement vector, averaged over the disk thickness, must satisfy equation [12]. Axial component $u_z^{(\rho)}(z)$, averaged over the electrode surface area, must satisfy the equation

$$\frac{\partial \sigma_{zz}^{(\rho)}(z)}{\partial z} + \rho_0 \omega^2 u_z^{(\rho)}(z) = 0, \quad (1)$$

which is obtained from the equation of steady axial oscillations after applying the averaging procedure to it [12]. Symbol $\sigma_{zz}^{(\rho)}(z)$ in equation (1) denotes normal stress $\sigma_{zz}(\rho, z)$, averaged over the area of the electrode-coated surface of the disk, i.e.

$$\sigma_{zz}^{(\rho)}(z) = \frac{2}{R^2} \int_0^R \rho \sigma_{zz}(\rho, z) d\rho. \quad (2)$$

Normal stresses $\sigma_{\rho\rho}^{(z)}(\rho)$, $\sigma_{\phi\phi}^{(z)}(\rho)$ and $\sigma_{zz}^{(\rho)}(z)$ are obtained by appropriately averaging the following expressions:

$$\begin{aligned} \sigma_{\rho\rho}(\rho, z) = & c_{11}^E \frac{\partial u_\rho(\rho, z)}{\partial \rho} + c_{12}^E \frac{u_\rho(\rho, z)}{\rho} + \\ & + c_{12}^E \frac{\partial u_z(\rho, z)}{\partial z} - e_{31} E_z(\rho, z), \quad (3) \end{aligned}$$

$$\begin{aligned} \sigma_{\phi\phi}(\rho, z) = & c_{12}^E \frac{\partial u_\rho(\rho, z)}{\partial \rho} + c_{11}^E \frac{u_\rho(\rho, z)}{\rho} + \\ & + c_{12}^E \frac{\partial u_z(\rho, z)}{\partial z} - e_{31} E_z(\rho, z), \quad (4) \end{aligned}$$

$$\begin{aligned} \sigma_{zz}(\rho, z) = & c_{12}^E \frac{1}{\rho} \frac{\partial}{\partial \rho} [\rho u_\rho(\rho, z)] + \\ & + c_{33}^E \frac{\partial u_z(\rho, z)}{\partial z} - e_{33} E_z(\rho, z). \quad (5) \end{aligned}$$

Axial component $D_z(\rho)$ of the electrical induction vector has the following notation

$$\begin{aligned} D_z(\rho) = & e_{31} \frac{1}{\rho} \frac{\partial}{\partial \rho} [\rho u_\rho(\rho, z)] + \\ & + e_{33} \frac{\partial u_z(\rho, z)}{\partial z} + \chi_{33}^\varepsilon E_z(\rho, z). \quad (6) \end{aligned}$$

From condition $\partial D_z(\rho)/\partial z = 0$, there follows representation of the $D_z(\rho)$ component which is physically equivalent to expression (6)

$$\begin{aligned} D_z(\rho) = & e_{31} \frac{1}{\rho} \frac{\partial}{\partial \rho} [\rho u_\rho^{(z)}(\rho)] + \\ & + \frac{e_{33}}{\alpha} [u_z(\rho, \alpha) - u_z(\rho, 0)] - \chi_{33}^\varepsilon \frac{U_0}{\alpha}. \quad (7) \end{aligned}$$

Subtracting relation (7) from expression (6), we obtain

$$\begin{aligned} \frac{e_{31}}{\rho} \frac{\partial}{\partial \rho} \left\{ \rho [u_\rho(\rho, z) - u_\rho^{(z)}(\rho)] \right\} + \\ + e_{33} \left\{ \frac{\partial u_z(\rho, z)}{\partial z} - \frac{1}{\alpha} [u_z(\rho, \alpha) - u_z(\rho, 0)] \right\} + \\ + \chi_{33}^\varepsilon \left[E_z(\rho, z) + \frac{U_0}{\alpha} \right] = 0. \quad (8) \end{aligned}$$

Averaging expression (8) over the disk thickness gives us

$$E_z^{(z)}(\rho) = -U_0/\alpha. \quad (9)$$

The averaging procedure (2) over expression (8) brings us to the conclusion that in the case of a thin disk, when $u_\rho(R, z) - u_\rho^{(z)}(R) \cong 0$, the axial component of the electric field strength vector averaged over the area of the electroded surface takes the following form

$$\begin{aligned} E_z^{(\rho)}(z) = & -\frac{U_0}{\alpha} - \\ & - \frac{e_{33}}{\chi_{33}^\varepsilon} \left\{ \frac{\partial u_z^{(\rho)}(z)}{\partial z} - \frac{1}{\alpha} [u_z^{(\rho)}(\alpha) - u_z^{(\rho)}(0)] \right\}. \quad (10) \end{aligned}$$

By averaging expressions (3) and (4) over the thickness of the disk, and considering definition (9), we obtain

$$\begin{aligned} \sigma_{\rho\rho}^{(z)}(\rho) = & c_{11}^E \frac{\partial u_\rho^{(z)}(\rho)}{\partial \rho} + c_{12}^E \frac{u_\rho^{(z)}(\rho)}{\rho} + \\ & + \frac{c_{12}^E}{\alpha} [u_z(\rho, \alpha) - u_z(\rho, 0)] + \frac{e_{31}}{\alpha} U_0, \quad (11) \end{aligned}$$

$$\begin{aligned} \sigma_{\phi\phi}^{(z)}(\rho) = & c_{12}^E \frac{\partial u_\rho^{(z)}(\rho)}{\partial \rho} + c_{11}^E \frac{u_\rho^{(z)}(\rho)}{\rho} + \\ & + \frac{c_{12}^E}{\alpha} [u_z(\rho, \alpha) - u_z(\rho, 0)] + \frac{e_{31}}{\alpha} U_0. \quad (12) \end{aligned}$$

The following estimate is valid for a thin disk: $u_z(\rho, \alpha) - u_z(\rho, 0) \cong u_z^{(\rho)}(\alpha) - u_z^{(\rho)}(0)$. Taking this fact into account, we get the following result:

$$\rho^2 \frac{\partial^2 u_\rho^{(z)}(\rho)}{\partial \rho^2} + \rho \frac{\partial u_\rho^{(z)}(\rho)}{\partial \rho} + \left[(\lambda^E R)^2 - 1 \right] u_\rho^{(z)}(\rho) = 0, \quad (13)$$

where $\lambda^E = \omega / \sqrt{c_{11}^E / \rho_0}$ is the wave number of the piezoceramic disk's radial vibrations in the high frequency range, when $\sigma_{zz}(\rho, z) \neq 0$. The solution to equation (13) is obvious

$$u_\rho^{(z)}(\rho) = C J_1(\lambda^E \rho), \quad (14)$$

where C denotes the frequency dependent constant to be determined.

Subjecting relation (5) to the averaging operation (2), and assuming at the same time that the estimate $u_\rho(R, z) \cong u_\rho^{(z)}(R)$ is valid for a thin disc, we arrive to the following result

$$\sigma_{zz}^{(\rho)}(z) \cong \frac{2c_{12}^E}{R} u_\rho^{(z)}(R) + c_{33}^D \frac{\partial u_z^{(\rho)}(z)}{\partial z} - \frac{e_{33}^2}{\chi_{33}^E \alpha} \left[u_z^{(\rho)}(\alpha) - u_z^{(\rho)}(0) \right] + \frac{e_{33}}{\alpha} U_0, \quad (15)$$

where $c_{33}^D = c_{33}^E (1 + K_{33}^2)$; $K_{33}^2 = e_{33}^2 / (\chi_{33}^E c_{33}^E)$ is square electromechanical coupling coefficient for the thickness vibration mode of a piezoceramic plate polarized over the thickness.

Substituting expression (15) into equation (1), we reduce it to the following form:

$$\frac{\partial^2 u_z^{(\rho)}(z)}{\partial z^2} + \gamma^2 u_z^{(\rho)}(z) = 0, \quad (16)$$

where $\gamma = \omega / \sqrt{c_{33}^D / \rho_0}$ is wave number of axial (thickness) vibrations of the piezoceramic disk. The solution to equation (16) is as follows:

$$u_z^{(\rho)}(z) = A \cos \gamma z + B \sin \gamma z, \quad (17)$$

where A and B are frequency dependent constants to be determined. A , B and C constants are determined from the boundary conditions

$$\sigma_{\rho\rho}^{(z)}(R) \cong \left[c_{11}^E \frac{\partial u_\rho^{(z)}(\rho)}{\partial \rho} + c_{12}^E \frac{u_\rho^{(z)}(\rho)}{\rho} \right] \Big|_{\rho=R} + \frac{c_{12}^E}{\alpha} \left[u_z^{(\rho)}(\alpha) - u_z^{(\rho)}(0) \right] + \frac{e_{31}}{\alpha} U_0 = 0, \quad (18)$$

$$\sigma_{zz}^{(\rho)}(z) \Big|_{z=\alpha; 0} = 0, \quad (19)$$

where relation (15) defines normal stress $\sigma_{zz}^{(\rho)}(z)$.

Substituting solutions (14) and (17) into conditions (18) and (19) brings us to the following system of linear algebraic equations:

$$\begin{aligned} Am_{11} + Bm_{12} + Cm_{13} &= -\frac{e_{31}U_0}{c_{12}^E} p_1, \\ Am_{21} + Bm_{22} + Cm_{23} &= -\frac{e_{31}U_0}{c_{12}^E} p_2, \\ Am_{31} + Bm_{32} + Cm_{33} &= -\frac{e_{31}U_0}{c_{12}^E} p_3, \end{aligned} \quad (20)$$

where $m_{11} = -\frac{1 - \cos \gamma \alpha}{\gamma \alpha}$; $m_{12} = \frac{\sin \gamma \alpha}{\gamma \alpha}$; $m_{13} = \xi_1 \left[J_0(\xi_3 \gamma \alpha) - \frac{1 - k^E}{\xi_3 \gamma \alpha} J_1(\xi_3 \gamma \alpha) \right]$; $\xi_1 = \sqrt{\frac{c_{11}^E c_{33}^D}{c_{12}^E}}$; $\xi_3 = \frac{R}{\alpha} \sqrt{\frac{c_{33}^D}{c_{11}^E}}$; $p_1 = 1$; $p_2 = \frac{e_{33} c_{12}^E}{e_{31} c_{33}^D}$; $m_{21} = \frac{K_{33}^2 (1 - \cos \gamma \alpha)}{1 + K_{33}^2} \frac{1}{\gamma \alpha} - \sin \gamma \alpha$; $m_{22} = -\frac{K_{33}^2 \sin \gamma \alpha}{1 + K_{33}^2} \frac{1}{\gamma \alpha} + \cos \gamma \alpha$; $m_{23} = \frac{2c_{12}^E \alpha}{c_{33}^D R} \frac{J_1(\xi_3 \gamma \alpha)}{\gamma \alpha}$; $m_{31} = \frac{K_{33}^2 (1 - \cos \gamma \alpha)}{1 + K_{33}^2} \frac{1}{\gamma \alpha}$; $m_{32} = -\frac{K_{33}^2 \sin \gamma \alpha}{1 + K_{33}^2} \frac{1}{\gamma \alpha} + 1$; $m_{33} = m_{23}$; $p_3 = p_2$.

The solutions to the system of equations (20) can be written in the following form:

$$A = -\frac{e_{31}U_0}{\gamma \alpha c_{12}^E} \frac{\Delta(A)}{\Delta_0}, \quad B = -\frac{e_{31}U_0}{\gamma \alpha c_{12}^E} \frac{\Delta(B)}{\Delta_0}, \quad C = -\frac{e_{31}U_0}{\gamma \alpha c_{12}^E} \frac{\Delta(C)}{\Delta_0},$$

where $\Delta(A)$, $\Delta(B)$, $\Delta(C)$ and Δ_0 are determinants of the following matrices:

$$\Delta(A) = \det \begin{vmatrix} p_1 & m_{12} & m_{13} \\ p_2 & m_{22} & m_{23} \\ p_3 & m_{32} & m_{33} \end{vmatrix};$$

$$\Delta(B) = \det \begin{vmatrix} m_{11} & p_1 & m_{13} \\ m_{21} & p_2 & m_{23} \\ m_{31} & p_3 & m_{33} \end{vmatrix};$$

$$\Delta(C) = \det \begin{vmatrix} m_{11} & m_{12} & p_1 \\ m_{21} & m_{22} & p_2 \\ m_{31} & m_{32} & p_3 \end{vmatrix};$$

$$\Delta_0 = \det \begin{vmatrix} m_{11} & m_{12} & m_{13} \\ m_{21} & m_{22} & m_{23} \\ m_{31} & m_{32} & m_{33} \end{vmatrix}.$$

Having defined A , B and C constants, we can write the averaged displacements $u_\rho^{(z)}(R)$, $u_z^{(\rho)}(\alpha)$ and $u_z^{(\rho)}(0)$ in an explicit form and define an expression for the $\Xi^\varepsilon(\omega)$ function [12] in an explicit form

$$\Xi^\varepsilon(\omega) = \frac{U_0}{\Delta_0} F^\varepsilon(\omega, \Pi),$$

where $F^\varepsilon(\omega, \Pi)$ is a function depending on the frequency and geometric and physical-mechanical parameters of the disk (Π symbol in the list of function arguments), the numerical values of which are given by the formula

$$\begin{aligned} F^\varepsilon(\omega, \Pi) &= \frac{2e_{31}^2 \alpha}{\chi_{33}^E c_{12}^E R} \Delta(C) \frac{J_1(\lambda^E R)}{\gamma \alpha} + \\ &+ \frac{e_{33} e_{31}}{\chi_{33}^E c_{12}^E} \left[-\Delta(A) \frac{(1 - \cos \gamma \alpha)}{\gamma \alpha} + \Delta(B) \frac{\sin \gamma \alpha}{\gamma \alpha} \right] + 1. \end{aligned}$$

In this case, the desired electrical impedance of the piezoceramic disk in the high-frequency range is given by the following expression

$$Z_{el}(\omega) = \frac{U_0}{-i\omega C_d^\varepsilon \Xi^\varepsilon(\omega)} = \frac{\Delta_0}{-i\omega C_d^\varepsilon F^\varepsilon(\omega, \Pi)}, \quad (21)$$

where $C_d^\varepsilon = \pi R^2 \chi_{33}^\varepsilon / \alpha$ is the dynamic electrical capacitance of a piezoceramic disk at high frequencies.

In other words, at the electromechanical antiresonance frequencies ω_a , under the condition of zero energy losses due to viscous friction in the material of the piezoceramic disk, its electrical impedance $Z_{el}(\omega)$ increases indefinitely, which eliminates the electric current in the circuit and corresponds to the conditions of an open electrical circuit.

Thus, in the high-frequency range, quite similar to the conditions observed in the medium-frequency range, it is possible to calculate the frequency dependence of the mechanical quality factor in both medium and high-frequency ranges by including mechanical quality factors and end-to-end electromechanical resonances into the calculations.

3 Discussion of the modelling results

In a real experiment, there are no zeros or infinities, since in real elastic materials there are always viscous friction losses. These losses can be calculated through parameter Q_m , which has the meaning of the mechanical quality factor of the material. The Q -factor is a dimensionless number, the value of which is inversely proportional to the energy losses in the oscillatory system per period. In ideal elastic bodies, where viscous friction entails no energy loss, $Q_m \rightarrow \infty$. In real objects, the Q_m quality factor has a finite value. Thus, the elasticity moduli $c_{\beta\lambda}^E(Q_m)$ read as follows [13]

$$c_{\beta\lambda}^E(Q_m) = c_{\beta\lambda}^E(1 + i/Q_m), \quad (22)$$

where $c_{\beta\lambda}^E$ is the static modulus of elasticity; $i = \sqrt{-1}$ is unit imaginary number.

Figure 2 presents the calculations for the modulus of the electrical impedance of the disk, which have been performed according to formula (21) with the following fixed parameter set: $c_{11}^E = 110 \text{ GPa}$; $c_{12}^E = 60 \text{ GPa}$; $c_{33}^E = 100 \text{ GPa}$; $e_{33} = 18 \text{ C/m}^2$; $e_{31} = -8 \text{ C/m}^2$ and $\chi_{33}^\varepsilon = 1400 \chi_0$; $\chi_0 = 8,85 \cdot 10^{-12} \text{ F/m}$ is dielectric constant; mechanical quality factor of the piezoceramics is $Q_m = 100$; piezoceramic density is $\rho_0 = 7400 \text{ kg/m}^3$. The thickness of the disc is $\alpha = 3 \cdot 10^{-3} \text{ m}$. Ratio R/α , which was set equal to 100; 50; 25; 12,5 and 6,25, is the varying parameter of the family of curves shown in Fig. 2. Numerical R/α ratio values are indicated in the figure field next to the corresponding curves. The values of the electrical impedance modulus $Z_{el}(\omega)$ normalized to the magnitude of the modulus

$Z_{el}(\omega_a)$ at the thickness antiresonance frequency ω_a are plotted along the ordinate axis in Fig. 2. The dimensionless wave number $\gamma\alpha$ is measured along the abscissa axis. With the disk parameter values specified above, the $\gamma\alpha = 1$ value corresponds to the cyclic frequency $f = v^D / (2\pi\alpha) = 219,1 \text{ kHz}$, where $v^D = \sqrt{c_{33}^D / \rho_0} = 4130 \text{ m/s}$ is the propagation speed of plane compression-tension waves along the electric polarization of the disk.

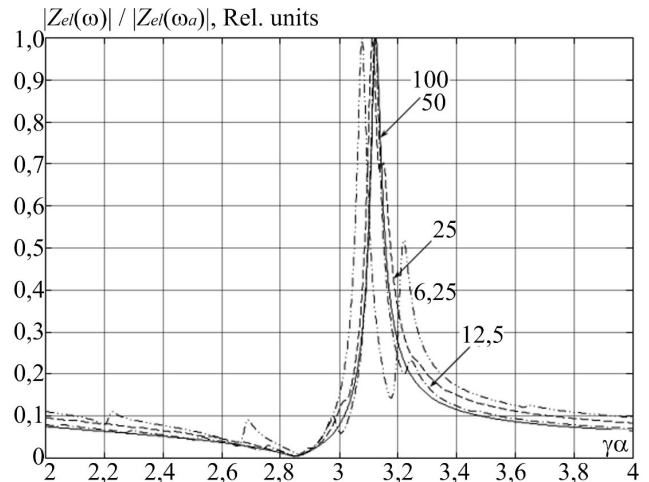


Fig. 2. Frequency-dependent change in the modulus of the electrical impedance of a piezoceramic disk in the vicinity of the first electromechanical antiresonance frequency through thickness

From the results shown in Fig. 2, it follows that with a significant change in the R/α ratio, the value of the dimensionless frequency of the first electromechanical antiresonance through thickness remains virtually unchanged. This is confirmed by the constructions shown in Fig. 3, where we have presented the calculations for expression $|Z_{el}(\omega)| / |Z_{el}(\omega_a)|$ in the immediate vicinity of the antiresonance frequency. The abscissa axis shows the values of the dimensionless frequency $\gamma\alpha$ in units of π -number, that is, $\gamma\alpha/\pi$ values. It is obvious that the maximum possible change in the dimensionless frequency of electromechanical antiresonance does not exceed $0,02\pi$. A similar conclusion is true for the influence of R/α on the value of the dimensionless frequency of the first thickness electromechanical resonance (Fig. 2), where $Z_{el}(\omega)$ module takes minimum values.

From the above results, the fact derives that radial displacement $u_\rho^{(z)}(R)$ of the material particles has virtually no effect on the numerical values of the frequencies of the first electromechanical resonance and antiresonance through the thickness. In other words, the numerical values of the electromechanical resonance and antiresonance frequencies are practically completely determined by axial displacements $u_z^{(p)}(z)$.

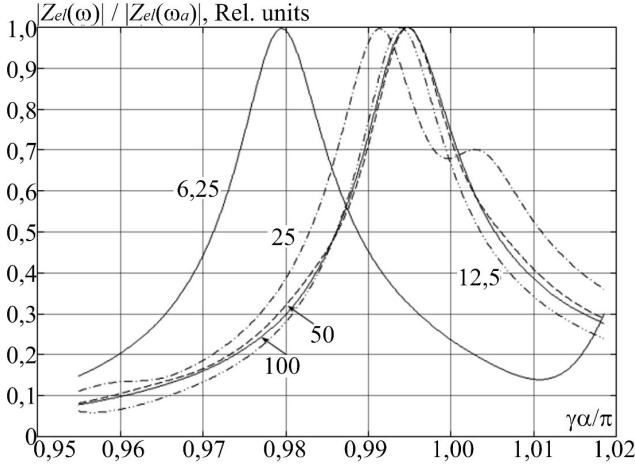


Fig. 3. Frequency-dependent change in the modulus of the electrical impedance of a piezoceramic disk in the vicinity of the first electromechanical antiresonance through thickness

Taking this circumstance into account, we can argue that in the high-frequency range, function $\Xi^\varepsilon(\omega)$ that determines the electrical impedance of the oscillating disk in the specified frequency range takes the following form

$$\Xi^\varepsilon(\omega) \cong \frac{e_{33}}{\chi_{33}^\varepsilon} \left[u_z^{(\rho)}(\alpha) - u_z^{(\rho)}(0) \right] - U_0. \quad (23)$$

When calculating the electrical impedance with formula (23), we will, naturally, omit some details of the frequency-dependent change in the function $Z_{el}(\omega)$. Nonetheless, we will preserve the primary characteristic, i.e., the numerical values of the frequencies of electromechanical resonance and antiresonance.

A and B constants included into the description of axial displacements $u_z^{(\rho)}(z)$ (see expression (17)) are determined from the boundary conditions (19), where normal stress $\sigma_{zz}^{(\rho)}(z)$ is given by the following expression

$$\begin{aligned} \sigma_{zz}^{(\rho)}(z) = & \\ = \gamma c_{33}^D & \left\{ -A \left[\sin \gamma z + \frac{K_{33}^2}{1 + K_{33}^2} \frac{(\cos \gamma \alpha - 1)}{\gamma \alpha} \right] + \right. \\ & \left. + B \left[\cos \gamma z - \frac{K_{33}^2}{1 + K_{33}^2} \frac{\sin \gamma \alpha}{\gamma \alpha} \right] + \frac{e_{33} U_0}{\gamma \alpha c_{33}^D} \right\}. \quad (24) \end{aligned}$$

Substituting the $z = \alpha$ and $z = 0$ values into expression (24) and equating the obtained results to zero, we obtain a system of linear algebraic equations from which A and B constants are determined in a unique way

$$\begin{aligned} A &= \frac{e_{33} U_0}{c_{33}^D} \frac{\operatorname{tg}(\gamma \alpha / 2)}{\gamma \alpha F^\varepsilon(\omega, \Pi)}, \\ B &= -A \cdot \operatorname{tg}(\gamma \alpha / 2), \end{aligned} \quad (25)$$

where

$$F^\varepsilon(\omega, \Pi) = 1 - \frac{K_{33}^2}{1 + K_{33}^2} \frac{\operatorname{tg}(\gamma \alpha / 2)}{(\gamma \alpha / 2)}. \quad (26)$$

Substituting expressions (25) into definition (17) of the axial displacements of material particles of the piezoceramic disk allows us to determine values $u_z^{(\rho)}(\alpha)$ and $u_z^{(\rho)}(0)$, which explicitly determine function $\Xi^\varepsilon(\omega)$, specified by (23). After this operation, the expression for calculating the electrical impedance $Z_{el}(\omega)$ takes the notation:

$$Z_{el}(\omega) = \frac{1}{i\omega C_d^\varepsilon} F^\varepsilon(\omega, \Pi). \quad (27)$$

From expression (27), it follows that when $\gamma \alpha / 2$ tends to the $\pi/2$ value from the left, the $F^\varepsilon(\omega, \Pi)$ function has positive values initially, then goes to zero, which corresponds to electromechanical resonance, and then tends to minus infinity. In the absence of energy loss due to viscous friction in the material of the piezoceramic disk ($Q_m \rightarrow \infty$) at $\gamma \alpha = \pi$, the electrical impedance is $Z_{el}(\omega_a) \rightarrow \infty$.

Figure 4a demonstrates the change of $F^\varepsilon(\omega, \Pi)$ function for $Q_m \rightarrow \infty$ and $K_{33}^2 = 0,262$ cases, which corresponds to the set of physical and mechanical parameters that served to calculate the curves in Fig. 2 and Fig. 3. Figure 4b shows the modulus of a complex-valued function $F^\varepsilon(\omega, \Pi)$ normalized to its maximum value when the mechanical quality factor of the disk material is $Q_m = 100$ and the dimensionless wave number $\gamma \alpha$ turns into a complex number $\gamma \alpha(1 - i/(2Q_m))$. Comparing the curves shown in Fig. 2 and Fig. 4b, we can conclude that a detailed calculation of the electrical impedance of an oscillating piezoceramic disk should be carried out by formula (21), and the numerical values of the resonance and antiresonance frequencies should be assessed with the function $F^\varepsilon(\omega, \Pi)$, which is given by expression (26).

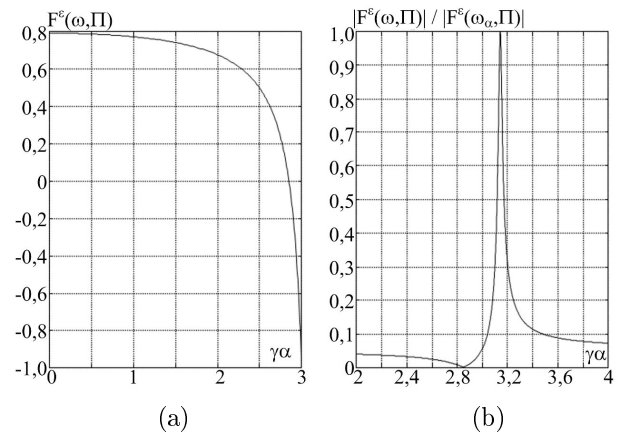


Fig. 4. Frequency-dependent change in function $F^\varepsilon(\omega, \Pi)$ in the absence of energy losses in the disk material (a) and for a material with a mechanical quality factor $Q_m = 100$ (b)

As a concluding stage in investigating the electrical impedance of a piezoceramic disk in a high-frequency range, consider its value at the frequency of the first electromechanical resonance.

In formula (26), the wave number γ and the square of the electromechanical coupling coefficient K_{33}^2

depend on the value of the mechanical quality factor Q_m . Along with that, $\gamma = \omega/v^D \cong \gamma^0 (1 - i/(2Q_m))$ and $K_{33}^2 = e_{33}^2/[\chi_{33}^\varepsilon c_{33}^E (1 + i/Q_m)]$, where γ^0 is the wave number of axial vibrations of the disk, determined without taking into account energy losses due to viscous friction. Obviously, parameter $\varepsilon = 1/(2Q_m) \ll 1$. Developing expression (27) at the frequency of the first electromechanical resonance as a series in powers of the small parameter ε , and limiting ourselves to the zero and first terms of the expansion, we obtain

$$Z_{el}(\omega_p) = \varepsilon \frac{K_{33}^2 \Psi(\omega_r)}{\omega_r C_d^\varepsilon (1 + K_{33}^2)}, \quad (28)$$

where $K_{33}^2 = \frac{e_{33}^2}{\chi_{33}^\varepsilon c_{33}^E}$; $\Psi(\omega_r) = \frac{2 \operatorname{tg}(\gamma^0 \alpha/2)}{(1 + K_{33}^2)(\gamma^0 \alpha/2)} + \frac{1 + \sin(\gamma^0 \alpha)/(\gamma^0 \alpha)}{\cos^2(\gamma^0 \alpha/2)}$.

Figure 5 contains graphs of the electrical impedance modulus $Z_{el}(\omega)$, calculated according to formula (21) in the immediate vicinity of the first electromechanical resonance frequency. The ordinate axis displays the values of the $Z_{el}(\omega)$ function modulus in ohms, the dimensionless frequency $\gamma\alpha = \omega\alpha/v^D$ is plotted along the abscissa axis, where $v^D = \sqrt{c_{33}^D/\rho_0}$ denotes the speed of plane compression-tension waves, to determine which we ignore losses in the piezoelectric. The calculations were performed for a disk with the ratio $R/\alpha = 12,5$. The rest of the parameters are indicated in the comments to Fig. 2. A variable parameter of the family of curves in Fig. 5 is the mechanical quality factor Q_m , which was assigned the values of 60, 80, 100 and 120 units. The quality factor values are indicated next to the corresponding curves. The graph clearly shows that the largest Q_m value corresponds to the smallest electrical impedance $Z_{el}(\omega_r)$ value which, as follows from formula (28), has positive real values, i. e. $|Z_{el}(\omega_r)| \equiv Z_{el}(\omega_r)$.

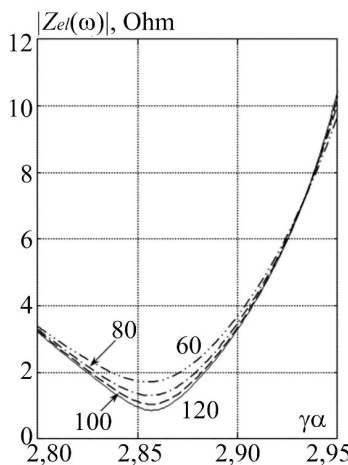


Fig. 5. Calculations of the electrical impedance modulus of the disk in the vicinity of the first electromechanical resonance frequency by formula (21)

Since value $Z_{el}(\omega_r)$ is measurable in a real experiment, expression (28) implies an estimate of the

mechanical quality factor Q_m at the frequency of the first thickness-through electromechanical resonance

$$Q_m = \frac{K_{33}^2 \Psi(\omega_r)}{2Z_{el}(\omega_r) \omega_r C_d^\varepsilon (1 + K_{33}^2)}. \quad (29)$$

Comparing the theoretical (calculated) and experimental data on the frequency dependence of the mechanical quality factor Q_m , it can be seen that the discrepancy between these data did not exceed $3 \cdot 10^{-3}$.

Note that the mechanical quality factor Q_m , found by [12] (we will denote this quality factor with $Q_m^{(\rho)}$) and the mechanical quality factor $Q_m^{(z)}$, determined by expression (29), are unequal. Moreover, inequality $Q_m^{(\rho)} > Q_m^{(z)}$ must be satisfied. Quite obviously, this state of affairs is due to energy losses. Due to viscous friction, energy losses increase with increasing frequency.

It follows from the theory of Lifshitz – Parkhomovsky – Merkulov that the damping coefficient β of ultrasound in a wide frequency range can be described by the expression

$$\beta \cong \delta_1 f^2 + \delta_2 f^4,$$

where δ_1 and δ_2 are structural parameters, the numerical values of which are determined by the average size of the grains of the material; f is the cyclic frequency.

The damping coefficient β and the mechanical quality factor Q_m are related, that is, in the medium frequency range $\beta = \lambda/(2Q_m^{(\rho)})$, and in the area of high frequencies $\beta = \gamma/(2Q_m^{(z)})$, where λ and γ are wave numbers of radial and thickness-through oscillating circular disks. Knowing the values of the mechanical quality factors $Q_m^{(\rho)}$ and $Q_m^{(z)}$ at the frequencies of the first and second radial, as well as the first and second thickness-through electromechanical resonances, it is possible to estimate the frequency dependence of the mechanical quality factor both in the medium and high frequency range. In addition, it is possible to form an estimate of the frequency dependence of the Q -factor in the transitional frequency range. The specified estimates are extremely important for mathematical modeling of functional devices of piezo electronics that operate in a wide frequency range [14, 15].

Conclusions

The purpose of the current study was to develop a mathematical model to accurately determine the electrical impedance of a piezoceramic disk oscillating in a high-frequency range. The model developed in this study incorporates both geometric and physical-mechanical parameters of the material to evaluate the behavior of the disk under varied conditions of electromechanical resonance and antiresonance. In particular, it has been found that in the antiresonance

range, the electrical impedance increases indefinitely under ideal conditions, which corresponds to the absence of electric current in the circuit and is critical when optimizing devices that operate in the high-frequency range.

Numerical calculations showed that the frequency dependence of the mechanical quality factor Q_m strongly correlates with the experimental data, ensuring high modeling accuracy (for example, the discrepancy between the calculated and experimental data did not exceed $3 \cdot 10^{-3}$). Therefore, the developed model is able to estimate energy losses due to viscous friction, as well as anticipate behavior of the piezoceramic material in transient modes. The second major finding was that the developed model makes it possible to analyze the frequency dependence of electrical impedance $Z_{el}(\omega)$, which is a significant factor in designing functional piezoelectric devices.

In addition, the simulation results revealed a minimal effect of radial displacements of material particles on the resonant frequencies ω_r , which simplifies the procedure for their analysis. Thus, in the high-frequency range, the main parameters of the disk are determined by axial displacements, which unlocks the potential for optimizing such mathematical models in practical applications.

Thus, the findings of the present study make several noteworthy contributions to improving mathematical models for analyzing the behavior of piezoceramic disks in the high-frequency range by creating a foundation for the further development of piezoelectric devices in acoustics, medicine, radio electronics and other industries, where the accuracy and stability of device operation are pivotal, and the obtained assessments and conclusions can build the basis for building new high-precision diagnostic systems.

The results presented by this study are being implemented under the experimental scientific and technical project titled “Development of an automated ultrasonic system for extracting plant raw materials to produce multi-nutrient functional drinks for rehabilitation and preventing post-traumatic stress disorders” (national registration number: 0124U000713, 2024-2025), which is under development at Cherkasy State Technological University.

References

- [1] Dong H., Zhu Z., Li Z. et al. (2024). Piezoelectric Composites: State-of-the-Art and Future Prospects. *JOM*, Vol. 76, pp. 340–352. DOI: 10.1007/s11837-023-06202-w.
- [2] Stankiewicz G., Dev C., Weichelt M. et al. (2024). Towards advanced piezoelectric metamaterial design via combined topology and shape optimization. *Struct Multidisc Optim.*, Vol. 67, article number 26. DOI: 10.1007/s00158-024-03742-w.
- [3] Shung K. K. (2015). *Diagnostic Ultrasound: Imaging and Blood Flow Measurements*, Second Edition (2nd ed). CRC Press, Washington, D.C. DOI: 10.1201/b18323.
- [4] Antonio Arnau Vives (2008). *Piezoelectric transducers and applications*. Springer Berlin, Heidelberg. DOI: 10.1007/978-3-540-77508-9.
- [5] Ammari H., Garnier J., & Jing W. (2012). Resolution and stability analysis in acoustoelectric imaging. *Inverse Problems*, Vol. 28, No. 8, 084005. DOI: 10.1088/0266-5611/28/8/084005.
- [6] Ammari H., Grasland-Mongrain P., Millien P., Seppecher L., & Seo J. K. (2015). A mathematical and numerical framework for ultrasonically-induced Lorentz force electrical impedance tomography. *Journal de Mathématiques Pures et Appliquées*, Vol. 103, Iss. 6, pp. 1390-1409. DOI: 10.48550/arXiv.1401.2337.
- [7] Gebauer B. & Scherzer O. (2008). Impedance-Acoustic Tomography. *SIAM J. Appl. Math.*, Vol. 69, Iss. 2, pp. 565–576. DOI: 10.1137/080715123.
- [8] Poplavko Y. M., Yakymenko Y. I. (2020). Large Parameters and Giant Effects in Electronic Materials. *Radioelectron. Commun. Syst.*, Vol. 63, pp. 289–298. DOI: 10.3103/S0735272720060023.
- [9] Oleynyk G. S. (2018). *Structure formation of ceramic materials*. Naukova dumka, Kyiv, Ukraine.
- [10] Antonyuk V.S., Bondarenko M.O., Bondarenko Yu.Yu. (2012). Studies of thin wear-resistant carbon coatings and structures formed by thermal evaporation in a vacuum on piezoceramic materials. *Journal of Superhard Materials*, Vol. 34, No. 4, pp. 248–255. DOI: 10.3103/S1063457612040065.
- [11] Aladwan I. M., Bazilo C., Faure E. (2022). Modelling and Development of Multisectional Disk Piezoelectric Transducers for Critical Application Systems. *Jordan Journal of Mechanical and Industrial Engineering*, Vol. 16, No. 2, pp. 275–282.
- [12] Petrishchev O. N. (2012). *Harmonic vibrations of piezoceramic elements. Part 1. Harmonic vibrations of piezoceramic elements in vacuum and the method of resonance-antiresonance*. Avers, Kiev, Ukraine.
- [13] Bazilo C. V. (2018). Principles and methods of the calculation of transfer characteristics of disk piezoelectric transformers. *Radio Electronics, Computer Science, Control*, No. 4, pp. 7-22. DOI: 10.15588/1607-3274-2018-4-1.
- [14] Bazilo C. (2020). Modelling of Bimorph Piezoelectric Elements for Biomedical Devices. In: Hu Z., Petoukhov S., He M. (eds) *Advances in Artificial Systems for Medicine and Education III. Advances in Intelligent Systems and Computing*, Vol. 1126, Springer, Cham, pp. 151–160. DOI: 10.1007/978-3-030-39162-1_14.
- [15] Nithya G., Sthuthi A., Chandrashekar N., et al. (2024). Modeling, Simulation, and Optimization of Piezoelectrically Actuated Dual-Axis MEMS Accelerometer for Seismic Sensing. *J. Vib. Eng. Technol.*, Vol. 12, pp. 5383–5395. DOI: 10.1007/s42417-023-01169-z.

Математичне моделювання електричного імпедансу п'єзокерамічного диска, що коливається в широкому діапазоні частот (Частина 3. Високі частоти)

Базіло К. В., Усик Л. М., Хиженяк Є. В., Жуйков Д. Б., Ярославський А. В.

У статті представлено результати математичного моделювання електричного імпедансу п'єзокерамічного диска, який коливається в широкому діапазоні високих частот. Основною метою дослідження є створення математичної моделі, яка враховує геометричні та фізико-механічні характеристики матеріалу для оцінки поведінки диска в умовах електромеханічного резонансу та антирезонансу. Особливу увагу приділено аналізу впливу радіальних і осьових зміщень матеріальних частинок на частотну залежність механічного коефіцієнта якості та електричного імпедансу диска. У науковій роботі також враховані специфічні ефекти, характерні для високочастотного режиму, з метою підвищення точності моделювання і забезпечення оптимальних технічних характеристик пристроїв. Отримана в роботі математична модель дозволяє отримувати оцінки частотної

залежності механічного коефіцієнта якості та динамічної електричної ємності в реальних умовах, зокрема з урахуванням енергетичних втрат через в'язке тертя. Числові розрахунки підтверджують високу кореляцію між теоретичними та експериментальними даними (розбіжність між ними не перевищила $3 \cdot 10^{-3}$), що дозволяє використовувати модель для проектування п'єзоелектричних пристроїв. Зокрема, встановлено, що частоти електромеханічного резонансу та антирезонансу практично не залежать від радіальних зміщень матеріальних частинок і визначаються лише осьовими компонентами. Розрахункова модель також забезпечує можливість оцінки електричного імпедансу у високочастотному діапазоні з точністю, що відповідає сучасним вимогам до проектування функціональних пристроїв п'єзоелектроніки. Отримані результати мають практичне значення для розроблення прецизійних елементів виробів військової техніки, високоточних сенсорів, ультразвукових генераторів, медичних діагностичних пристроїв та інших технологічних систем, що використовують п'єзоелектричні матеріали.

Ключові слова: електричний імпеданс; п'єзокерамічний диск; високі частоти; математичне моделювання; добротність; електромеханічний резонанс